Journal of Mechanics Engineering and Automation 7 (2017) 171-179
doi: 10.17265/2159-5275/2017.04.001

Enhancement of DC-Link Protection of PMSG Based Wind Turbine under Network Disturbance by Using New Buck Controller System

Linda Sartika, Atsushi Umemura, Rion Takahashi and Junji Tamura

Department of Electrical and Electronic Engineering, Kitami Institute of Technology (KIT), Hokkaido 090-8507, Japan

Abstract: Protection system for DC-link circuit of back-to-back converter of PMSG (Permanent Magnet Synchronous Generator) based wind turbine is essential part for the system to ride through a network fault in grid system. Voltage on the DC-link circuit can be increased significantly due to power unbalance between stator side converter and grid side converter. Increase of DC-link circuit voltage can lead to a damage of IGBT of the converter and control system failure. In this paper performance enhancement of DC-link protection of PMSG based wind turbine by using new control system of buck converter is proposed. The buck converter is used to control supplied voltage of a breaking resistor to dissipate energy from the wind generator during network disturbance. In order to investigate effectiveness of the proposed DC-link protection system, fault analysis is performed in the simulation study by using PSCAD/EMTDC software program. In addition, comparative analysis between the proposed protection system and the conventional protection system using DC chopper is also performed.

Key words: Wind farm, variable speed wind turbine, permanent magnet synchronous generator, buck controller.

1. Introduction

In many countries utilization of wind power is being encouraged by way of government's policy to establish the real commercial generation projects [1, 2]. Large scale of wind farms are planned in many countries not only for reducing the production of CO_2, SO_2 and NO_X but also for economic competition [2].

Over recent years, PMSG (Permanent Magnet Synchronous Generator) based variable speed wind turbine has become one of the most popular types of wind turbine generator. In this concept, PMSG is directly driven by a wind turbine without gear and is connected to the AC power grid through the power converter. Permanent magnet machines are characterized as having large air gaps, which reduce flux linkage even in machines with multi-magnetic poles [3-6]. PMSG system equipped with full rating power electronic converters has strong fault ride through capability during a network disturbance.

Currently, most of PMSG system studies consider normal operation, for example, realization of maximum power point tracking. Studying on the PMSG system protection is not so much [7], meanwhile, enhancement of FRT (fault ride-through) capability is required for operating of wind farm. The wind farm should stay online during and after a network disturbance [8]. Therefore, enhancement of protection system of the wind generator is very important to be studied. When a fault occurs in the grid, a voltage dip appears at the terminal of wind generator and then the active power delivered to the grid is also reduced. As the generator side converter is decoupled with the grid, generator continues to generate the active power and thus the DC-link voltage increases due to the energy unbalance between the generator side converter and the grid side converter.

Usually, a simple DC chopper with a braking resistance is inserted into the DC-link circuit to

Corresponding author: Linda Sartika, M.Eng., research fields: dynamic stability and control of power system including large scale wind generator.

dissipate the active power produced by PMSG in such a way that the active power balance in the DC-link circuit is maintained [4, 6, 9]. However, it can have a problem if the active power coming from the PMSG is not balanced against the capacity of braking resistor. This is because the capacity of resistor in the protection system with a simple DC chopper is constant (uncontrolled). In order to solve the problem new topology of DC-link protection of PMSG by using buck converter is proposed in this paper.

2. PMSG Based Wind Turbine

A configuration of PMSG based wind turbine is shown in Fig. 1. The wind turbine directly drives the rotor of PMSG without a gear box. The stator winding of PMSG is connected to the grid system through fully rated power of back-to-back converter and a step up transformer (TR). The back-to-back converter consists of SSC (stator side converter) and GSC (grid side converter) linked by DC circuit. Typically, SSC controls active power (P_s) and reactive power (Q_s) of the generator by controlling its stator current (I_s). On the other hand, grid side converter maintains the DC-link voltage (V_{dc}) across of DC capacitor (C_{dc}) to be constant and controls the reactive power (Q_g) injected to grid system by controlling the converter grid current (I_g) [10]. Both converters are constructed from IGBTs circuit of which switching is controlled by PWM (pulse wide modulation) technique. SSC is operated under variable frequency depending on the rotational speed of generator (ω_r) and GSC is operated under constant frequency depending on the grid system (50 Hz or 60 Hz). In order to synchronize frequency between the grid side converter output and the grid system, PLL (phase lock loop) is used [11]. The PLL generates a phase output signal (θ_g). A pitch controller is equipped with the wind turbine to control pitch angle of wind turbine blades (β) when the rotational speed increases over the generator's maximum speed. DC-link protection circuit is installed parallel with the DC capacitor. The DC protection circuit limits the transient over voltage of the DC-link circuit due to network disturbance such as a short circuit. The DC-ink protection protects both IGBTs of back-to-back converter and DC capacitor.

2.1 Aerodynamic Model

The mathematical model expressing mechanical power extraction from wind can be written as follows [12]:

$$P_w = 0.5\rho\pi R^2 V_w^3 C_p(\lambda,\beta) \tag{1}$$

where, P_w is the captured wind power (W), ρ is the air density (kg/m^3), R is the radius of rotor blade (m), V_w is wind speed (m/sec), and C_p is the power coefficient.

The power coefficient is depending on tip speed ratio (λ) and blade pitch angle (β) of the wind turbine. The power coefficient of the turbine can be obtained as follows:

$$C_p(\lambda,\beta) = c_1\left(\frac{c_2}{\lambda_i} - c_3\beta - c_4\right)e^{\frac{-c_5}{\lambda_i}} + c_6\lambda \tag{2}$$

with

$$\frac{1}{\lambda_i} = \frac{1}{\lambda - 0.08\beta} - \frac{0.035}{\beta^3 + 1} \tag{3}$$

and

$$\lambda = \frac{\omega_r R}{V_w} \tag{4}$$

The characteristic coefficients of wind turbine, c_1 to c_6, are $c_1 = 0.5176$, $c_2 = 116$, $c_3 = 0.4$, $c_4 = 5$, $c_5 = 21$ and $c_6 = 0.0068$ [13], and ω_r is rotational speed of turbine in rad/sec.

The C_p-λ characteristic for different values of the pitch angle β is shown in Fig. 2a. The maximum value of C_p ($C_{p\_opt} = 0.48$) is achieved for $\beta = 0^\circ$ and $\lambda = 8.1$. This value of λ is defined as the optimal value (λ_{opt}). Fig. 2b depicts the turbine output power as a function of the rotor speed with the blade pitch angle $\beta = 0^\circ$.

In variable speed wind turbines, the rotational speed of wind turbine is controlled to follow the MPPT (maximum power point trajectory) as follows:

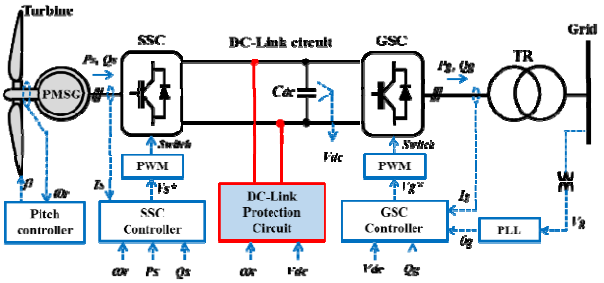

Fig. 1 Configuration of PMSG based wind turbine.

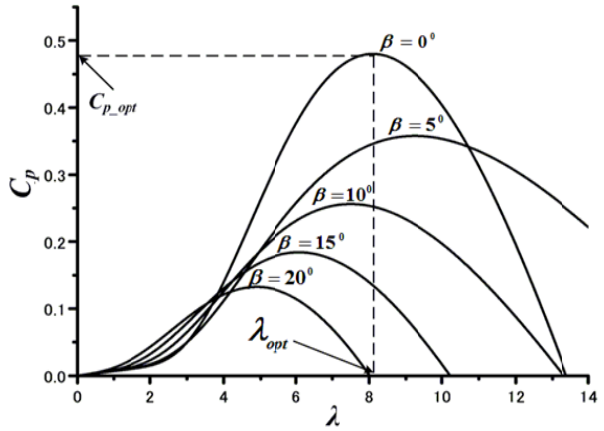

(a) Cp-λ characteristic for different pitch angle

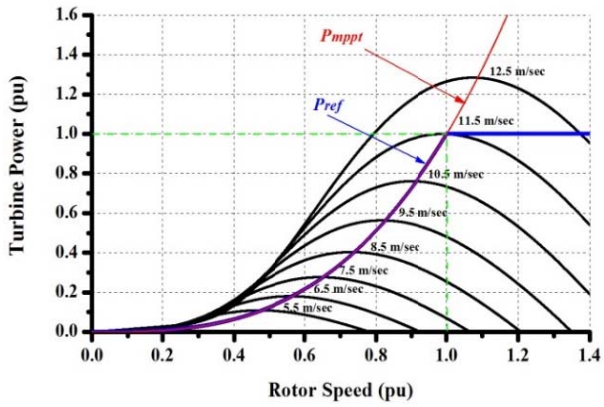

(b) Power characteristic

Fig. 2 Characteristic wind turbine.

$$P_{mppt} = 0.5\rho\pi R^2 \left(\frac{\omega_r R}{\lambda_{opt}}\right)^3 Cp_{opt} \quad (5)$$

2.2 Mechanical Model

The rotating mass of mechanical wind turbine system consists of wind turbine rotor, generator, and a gear box. It is known that the single rotating mass or one-lump mass is sufficient as shaft model for analysing the impact of wind speed fluctuations [14, 15]. When the effect of a severe network disturbance in the power system is analysed, however, at least two mass shaft model should be considered [16, 17]. Wind turbine rotor, generator, and a gear box can be represented as two mass inertia model. State space equations of the two mass drive train model are expressed as follows:

$$\frac{d}{dt}(\delta_t - \delta_g) = (\omega_t - \omega_g) \quad (6)$$

$$\frac{d}{dt}\omega_t = \left(\frac{1}{2H_t}\right)\left(T_m - D(\omega_t - \omega_g) - K(\delta_t - \delta_g)\right) \quad (7)$$

$$\frac{d}{dt}\omega_g = \left(\frac{1}{2H_g}\right)\left(D(\omega_t - \omega_g) + K(\delta_t - \delta_g) - T_e\right) \quad (8)$$

where,

H_t, H_g: Moments of inertia of wind turbine rotor and generator;

T_m, T_e: Wind turbine aerodynamic and electromagnetic torques;

ω_t, ω_g: Wind turbine rotor and generator speeds;

δ_t, δ_g: Angular positions of rotor and generator;

D_{shaft}: Damping coefficient;

K_{shaft}: Spring constants.

2.3 Pitch Control Model

Fig. 3 depicts a pitch controller system of wind turbine [14, 18]. The pitch controller of variable speed wind turbine usually regulates rotational speed of the rotor not to be over its setting value. The control loop of the pitch actuator is represented by a first-order transfer function with time constant (T_β) and the pitch rate limiter. In this model, the blade pitch angle of wind turbine is kept to zero degree when the rotational speed is less than the setting value (ω_{set} = 1.21 pu).

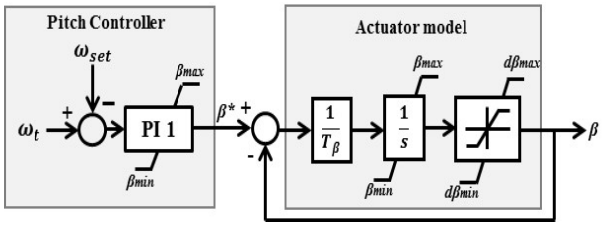

Fig. 3 Pitch controller model.

2.4 PMSG (Permanent Magnet Synchronous Generator) Model

Differential equations of permanent magnet synchronous machine can be expressed in the DQ rotor reference frame, where all quantities in the rotor reference frame are referred to the stator [13, 19]. The equations are expressed as follows:

$$Lds\frac{di_{ds}}{dt} = V_{ds} - R_s i_{ds} + \omega_s L_{qs} i_{qs} \quad (9)$$

$$Lqs\frac{di_{qs}}{dt} = V_{qs} - R_s i_{qs} + \omega_s L_{ds} i_{ds} - \omega_s \varphi_m \quad (10)$$

where, L_{ds} and L_{qs} are inductances of stator winding, R_s is the stator winding resistance, V_{ds} and V_{qs} are stator voltages, I_{ds} and I_{qs} are stator currents, ω_s is angular frequency of the stator, and ψ_m is the permanent magnet flux linkage.

2.5 Converter Controller System

Block diagram of SSC controller is depicted in Fig. 4. The aim of the SSC controller is to control active and reactive power output of PMSG. The active power and reactive power of the PMSG are controlled by the q-axis current (Isq) and the d-axis (Isd) current, respectively. The active power reference (Ps*) is obtained by MPPT controller. The reactive power reference (Qs*) is set to zero for unity power factor operation.

Fig. 5 shows a block diagram of the GSC controller. The controller is used to control the reactive power output of GSC and DC-link voltage by controlling the d-axis (I_{gd}) and the q-axis (I_{gq}) output currents of GSC. The reactive power reference (Q_{g*}) is set to zero and the DC voltage reference (V_{dc*}) is set to 3.0 kV (rated value).

3. DC-Link Protection System

During a network disturbance like a short circuit fault, output power of the PMSG decreases at the grid side converter and then over voltage can appear in DC-link circuit of the back-to-back power converter of PMSG. During a fault condition, the DC-link voltage can suddenly increase due to the energy imbalance between the stator side converter and the grid side converter. The voltage increase can be controlled by inserting a braking resistor in the DC-link circuit to dissipate the excess energy through a power electronic switch as shown in Fig. 6. However, dissipated energy in the braking resistor cannot be controlled, and hence, energy imbalance between SSC and GSC can still appear. This can appear due to the imbalance between the output power

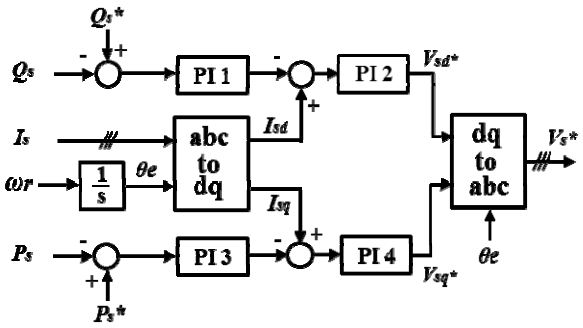

Fig. 4 Stator side converter controller system.

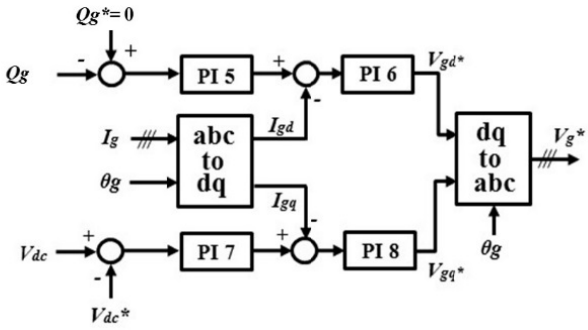

Fig. 5 Grid side converter controller system.

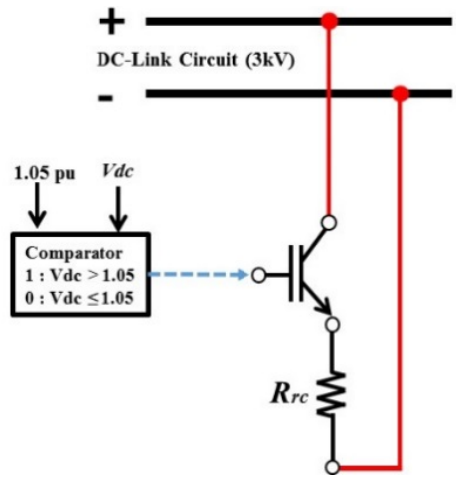

Fig. 6 Conventional DC-link protection system.

from the generator and the power capacity of the resistor.

The detailed control scheme of the DC-link protection system proposed in this paper is shown in Fig. 7. The protection system consists of main switch circuit and buck converter circuit. Main switch circuit is used to activate the DC-link protection when DC-link circuit voltage increases more than 1.05 pu due to a fault in the grid system. The buck converter is used to control DC voltage (V_{rc}) across the breaking resistance (R_{rc}) depending on power generated from the PMSG (P). The power output of PMSG is determined from its rotational speed through maximum power point tracking controller. By using the information, generated power from PMSG and consumed power in the breaking resistance can be balanced, and then, dynamic stability of the PMSG can be enhanced.

Fig. 8 illustrates the basic principle of the buck-chopper composed of IGBT as a switch breaker [20]. During the period T_{on} the chopper is operated, and the source voltage will be connected to the load (R_{rc}) terminals. Furthermore, during the period T_{off}, the chopper is off, the current i_0 in R_{rc} will flow into the commutation diode (D_F), the load terminals are connected briefly through D_F, and V_{rc} becomes zero. Thus, the average value of the DC voltage at the load can be determined by the following equation.

$$e_o = V_{dc}\alpha \tag{11}$$

$$\alpha = D = \left(\frac{T_{on}}{T_{on} + T_{off}}\right) = \left(\frac{T_{on}}{T}\right) = f \cdot T_{on} \tag{12}$$

where,

e_0: DC voltage on the load;

V_{dc}: Voltage source;

α, D: Duty cycle;

T_{on}: Period of switch-on;

T_{off}: Period of switch-off;

f: Frequency;

T: Period.

If a fault occurs in the grid system, the grid side converter has a voltage dip on the grid side voltage. Therefore power sent from the converter to the grid is influenced. After the disturbance is cleared, the converter voltage returns to the normal, and then the active power will be supplied to the grid again. Power transferred from the GSC to the grid is given by Eq. (13) [21].

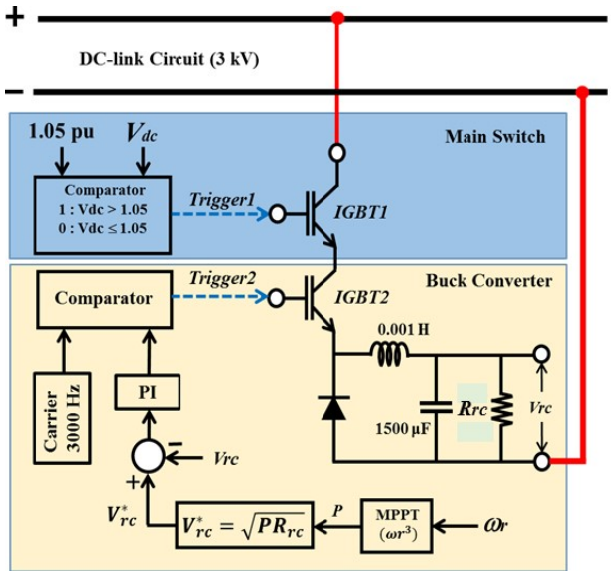

Fig. 7 Proposed DC-link protection system.

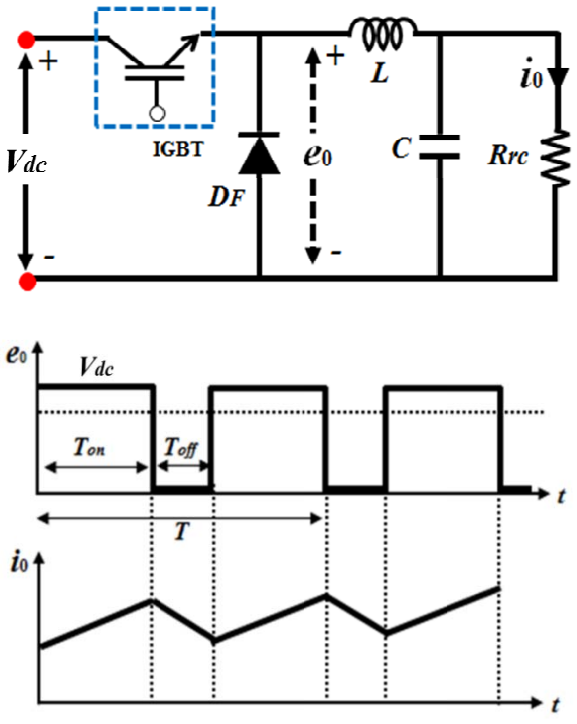

Fig. 8 Basic chopper step-down circuit.

$$P_{cg} = \frac{V_c * V_g}{X_{ph}} \sin(\delta_c - \delta_g) \quad (13)$$

where,

P_{cg}: Power transferred from the converter to the grid;

V_c, δ_c: Converter terminal voltage (magnitude and phase of the fundamental component);

V_g, δ_g: Grid terminal voltage (magnitude and phase of the voltage grid);

X_{ph}: Reactance between V_c and V_g.

When V_g decreases to 0, the active power cannot be transferred to the grid, and then over voltage as given in Eq. (14) appears in the DC-link circuit.

$$V_{dc} = \sqrt{\frac{2}{C_{dc}} \int (P_{WT} - P_{cg})\, dt} \quad (14)$$

DC over-voltage can be controlled within a safe level if the excess power is discarded in several ways, for example, chopper controlled resistor. Resistor of the chopper can be determined as follows:

$$R_{rc} = \frac{V_{rated}^2}{P_{rated}} \quad (15)$$

$$I_{chop} = \frac{1.05\ V_{rated}}{R_{chop}} = \frac{1.05\ P_{rated}}{V_{chop}} = 1.05\ I_{rated} \quad (16)$$

4. Simulation Analysis

4.1 Power System Model

The power system model considered in this analysis is shown in Fig. 9. A wind farm with power capacity of 25 MW composed of five PMSGs each rated at 5 MW is connected to a large power system through a 33 kV/66 kV, 25 MVA main transformer and 66 kV double circuit transmission line. The grid frequency is 50 Hz and system base is 25 MVA.

The parameters of PMSG based wind turbine are presented in Table 1. Temporary three-line table to ground fault (3 LG) for 5 cycles (0.1 sec) is considered as network disturbance. The fault occurs at 1.0 sec. In this study, the different wind speed data are applied to the each wind turbine as shown in Fig. 9.

4.2 Simulation Results

The proposed controller has been investigated through simulation analyses performed by using PSCAD/EMTDC. Two cases are considered as scenarios to confirm the effectiveness of the proposed control system. In Case 1, the proposed controller system shown in Fig. 7 is used for DC-link protection system. In Case 2, the DC link protection is performed by using conventional system shown in Fig. 6. In both scenarios wind speeds for each wind generator are kept constant to the values shown in Fig. 9 and value of R_{rc} is set at 1.0 pu.

Comparative simulation analysis of PMSG's dynamic responses has been performed between the proposed method (Case 1) and conventional method (Case 2), and the results are shown in figures.

Figs. 10-12 show the responses of DC-link circuit voltage during (3 LG) three lines to ground fault. In the simulation analysis, wind speeds of PMSG1, PMSG3, and PMSG5 are 12 m/sec, 11 m/sec, and 10 m/sec, respectively. It is seen from the figures that excess DC-link voltage can be well controlled in the proposed method. Figs. 13-15 show the rotor speed responses of PMSGs for Case 1 and Case 2, from which it is seen that transient oscillation of the rotor

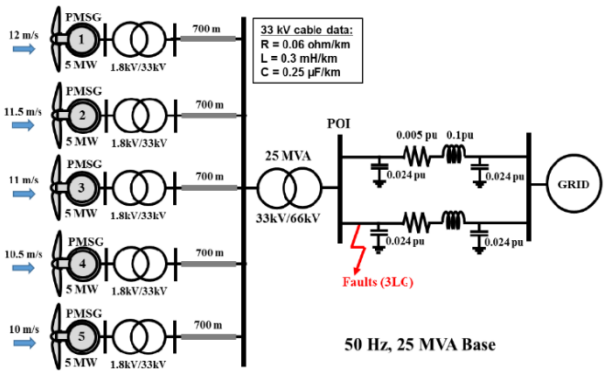

Fig. 9 Power system model.

Table 1 Parameters of PMSG based wind turbine.

Generator parameter	Value	Drive train parameter	Value
Power	5 MW	*Hg*	0.45 s
Voltage	1,800 V	*Ht*	3.0 s
Frequency	20 Hz	*D*	1.5
R_s	0.017 pu	*K*	296
L_{ds}	0.96 pu		
L_{qs}	0.76 pu		
ψ_m	1.4		

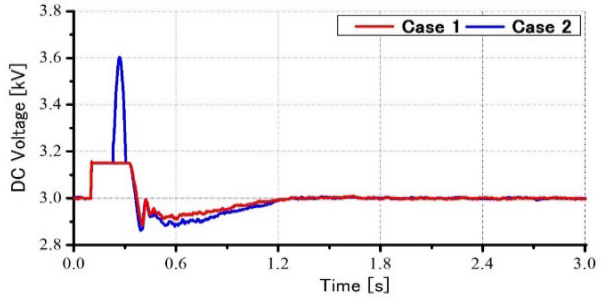

Fig. 10 DC-link voltage response of PMSG1 (12 m/sec).

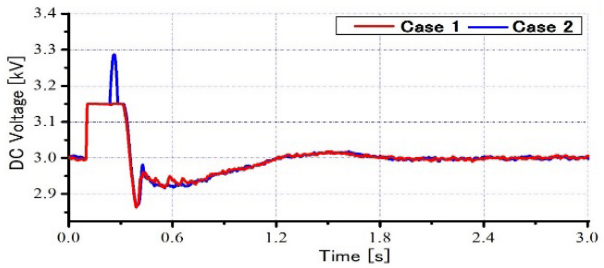

Fig. 11 DC-link voltage response of PMSG3 (11 m/sec).

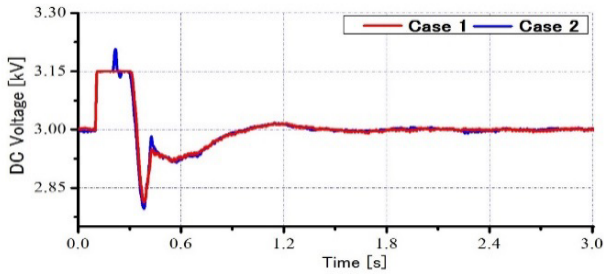

Fig. 12 DC-link voltage response of PMSG5 (10 m/sec).

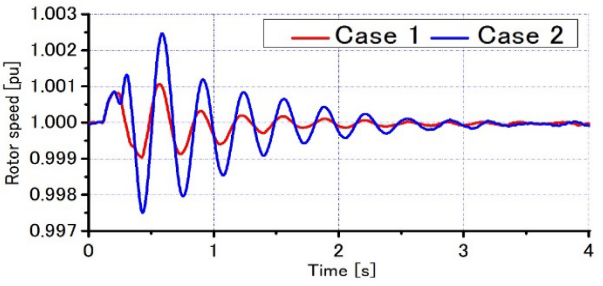

Fig. 13 Rotor speed response of PMSG1 (12 m/sec).

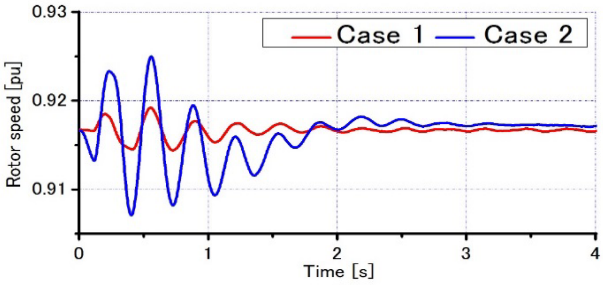

Fig. 14 Rotor speed response of PMSG3 (11 m/sec).

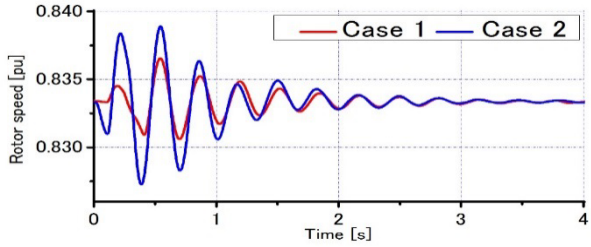

Fig. 15 Rotor speed response of PMSG5 (10 m/sec).

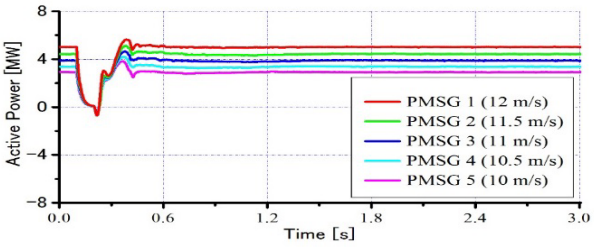

Fig. 16 Active power output of PMSGs in Case 1 (proposed method).

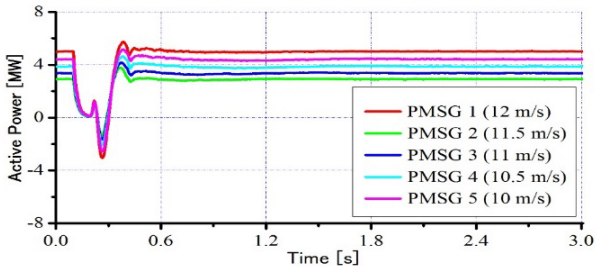

Fig. 17 Active power output of PMSGs in Case 2 (conventional method).

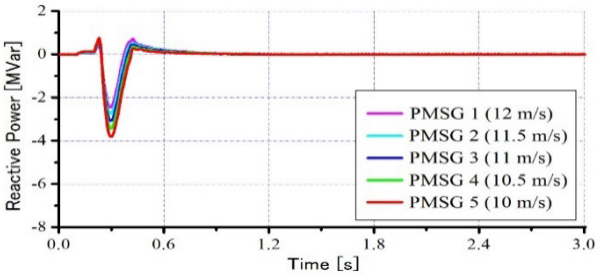

Fig. 18 Reactive power output of PMSGs in Case 1 (proposed method).

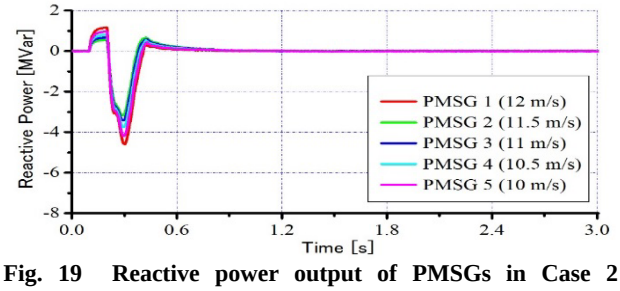

Fig. 19 Reactive power output of PMSGs in Case 2 (conventional method).

speed can be well controlled in the proposed method. Figs. 16-19 show responses of active and reactive power outputs of all the PMSGs, respectively. From the figures, it is seen that power drop and power swing during the fault can be reduced more significantly in the proposed method than the conventional method.

5. Conclusions

A new DC-link protection scheme using buck converter has been proposed for permanent magnet wind generator and its performance under network disturbance condition has been investigated through simulation analyses using PSCAD/EMTDC. Comparative simulation analysis has been performed for severe three-line to ground (3 LG) fault between the proposed DC-link protection system and the conventional protection system. From the simulation results, it is shown that the proposed method can control well the DC-link voltage as well as other dynamic responses of PMSG such as rotor speed and active power output. Therefore it can be concluded that the dynamic performance of PMSG can be enhanced by the proposed DC-link protection system.

Acknowledgements

The authors thank Dr. Marwan Rosyadi in Hitachi Power Solutions Co., Ltd., for his valuable comments and encouragement.

This study was supported by the Grant-in-Aid for Scientific Research (B) from the Ministry of Education, Science, Sports and Culture of Japan.

References

[1] "Fukushima Floating Offshore Wind Farm Demonstration Project (Fukushima FORWARD)." Accessed June 22, 2015. http://www.fukushima-forward.jp/english/.

[2] Author the Global Wind Energy Council (GWEC). Global Wind Report 2015, April 2016. [Online]. Available: http://www.gwec.net.

[3] Papaefthimiou, S. B., and Papathanassiou, S. A. 2006. "Simulation and Control of a Variable Speed Wind Turbine with Synchronous Generator." In *Proceedings of the CD Rec. XVII Int. Conf. Electrical Machines (ICEM 2006),* Chania, Crete Island, Greece.

[4] Muyeen, S. M., Takahashi, R., Murata, T., Tamura, J., and Ali, M. H. 2007. "Transient Stability Analysis of Permanent Magnet Variable Speed Synchronous Wind Generator." In *Proceedings of the Proc. Int. Conf. Electrical Machines and Systems 2007 (ICEMS 2007),* Seoul, Korea, Oct. 288-93.

[5] Hansen, A. D., and Michalke, G. 2008. "Modelling and Control of Variable Speed Multi-pole Permanent Magnet Synchronous Generator Wind Turbine." *Wind Energy* 11 (5): 537-54.

[6] Muyeen, S. M., Takahashi, R., Murata, T., and Tamura, J. 2010. "A Variable Speed Wind Turbine Control Strategy to Meet Wind Farm Grid Code Requirements." *IEEE Transactions on Power Systems* 25 (1).

[7] Conroy, J. F., and Watson, R. 2007. "Low-Voltage Ride-through of a Full Converter Wind Turbine with Permanent Magnet Generator." *IET Renew. Power Gener.* 1 (3): 182-9.

[8] Jauch, C., Matevosyan, J., Ackermann, T., and Bolik, S. 2005. "International Comparison of Requirements for Connection of Wind Turbines to Power Systems." *Wind Energy* 8 (3): 295-306.

[9] Rosyadi, M., Muyeen, S. M., Takahashi, R., and Tamura, J. 2013. "Stabilization of Fixed Speed Wind Generator by Using Variable Speed PM Wind Generator in Multi-machine Power System." *Electrical Machines and Systems (ICEMS)* 2 (1): 111-9.

[10] Fernandes, L. M., Garcia, C. A., and Jurado, F. 2010. "Operating Capability as a PQ/PV Node of a Direct-Drive Wind Turbine Based on a Permanent Magnet Synchronous Generator." *Journal of Renewable Energy* 35: 1308-18.

[11] "PSCAD/EMTDC User's Manual." *Manitoba HVDC Research Center,* Canada, 1994.

[12] Heier, S. 1998. *Grid Integration of Wind Energy Conversion Systems.* John Wiley & Sons Ltd.

[13] MATLAB Documentation Center, Accessed November 3, 2012. [Online] http://www.mathworks.co. jp/jp/help/.

[14] Achilles, S., and Poller, M. "Direct Drive Synchronous Machine Models for Stability Assessment of Wind Farm." http://www.digsilent.de/Consulting/Publications/DirectDrive_Modeling.pdf.

[15] Miller, N. W., Sanchez-Gasca, J. J., Price, W. W., and Delmerico, R. W. 2003. "Dynamic Modeling of GE 1.5 and 3.6 MW Wind Turbine-Generators for Stability Simulations." Presented at *Power Engineering Society General Meeting,* Toronto.

[16] Anderson, P. M. 1994. *Subsynchronos Resonance in Power System.* New York: IEEE Pres.

[17] Kundur, P. 1986. *Power System Stability and Control.* London: McGraw-Hills.

[18] Gonzalez-Longatt, F. M., Wall, P., and Terzija, V. 2011.

"A Simplified Model for Dynamic Behavior of Permanent Magnet Synchronous Generator for Direct Drive Wind Turbines." *Power Tech*, Norway.

[19] Sances, A. G., Molina, M. G., and Rizzato Lede, A. M. 2012. "Dynamic Model of Wind Energy Conversion System with PMSG-Based Variable-Speed Wind Turbine for Power System Studies." *International Journal of Hydrogen Energy* 37 (13): 10064-9.

[20] Mohan, N., Undeland, T. M., and Robbins, W. P. 2003. *Power Electronics Converters, Applications and Design.* Hoboken, NJ: John Wiley & Sons.

[21] Chaudhary, S. K., Teodorescu, R., Rodriguez, P., and Kjaer, P. C. 2009. "Chopper Controlled Resistors in VSC-HVDC Transmission for WPP with Full-Scale Converters." In *Proc. IEEE PES/IAS Conference on Sustainable Alternative Energy (SAE)*, 1-8.